Interval: Indonesian Journal of Mathematical Education
Vol. 3, No. 1, June 2025, pp. 1~12
ISSN: 3021-7857, DOI: 10.37251/ijome.v3i1.1613

Numerical Analysis of Flow Through Venturimeter With Variation of Neck Size to Determine Velocity Coefficient and Pressure Drop

Zakaria Gaber Henawy Beshay[1], Sokunthea Sin[2], Waleed A. Raja[3]
[1]Department of Science Education, Math Education, Assiut University, Asyut, Egypt
[2]Lecturer of Mathematics, Mathematics Education, Phnom Penh Teacher Education College, Cambodia
[3]Student of Mathematics Education, Syracuse University, United States

Article Info

Article history:

Received Feb 27, 2025
Revised Mar 11, 2025
Accepted Apr 29, 2025
Online First May 1, 2025

Keywords:

Numerical Simulation
Pressure Drop
Reynolds Number
Velocity Coefficient
Venturimeter

ABSTRACT

Purpose of the study: This study aims to analyze the effect of variations in the size of the venturimeter neck on the velocity coefficient and pressure drop using a numerical simulation method. By understanding the relationship between these parameters, this study can provide insight into more accurate fluid flow measurements.

Methodology: The method used in this study is numerical simulation using SolidWorks 2014 software. The simulated venturimeter model has a neck length variation of 20 mm and 30 mm, with a throat diameter of 10 mm. The fluid used is water with a temperature of 25°C, and the simulation is carried out in the Reynolds number (Re) range of 1000 to 5000.

Main Findings: The results of the study showed that the greater the velocity of the incoming fluid, the Reynolds number, flow rate, and pressure drop also increased. In addition, the difference in the length of the venturimeter neck affects the pressure drop, where the venturimeter with a longer neck experiences a greater pressure drop due to the longer duration of the fluid flow. The resulting velocity coefficient is also influenced by the velocity of the incoming fluid, where the higher the velocity, the greater the flow rate value.

Novelty/Originality of this study: The novelty in this research lies in the numerical approach in analyzing the relationship between the venturimeter neck size and the velocity coefficient and pressure drop. This approach allows faster and more efficient calculations compared to conventional experimental methods, thus contributing to the development of more accurate and applicable fluid flow measurement techniques.

This is an open access article under the CC BY license

Corresponding Author:
Zakaria Gaber Henawy Beshay,
Department of Science and Education, Math Education, Assiut University, Libraries Road, Markaz El-Fath, Assiut Governorate, 71515, Egypt
Email: zakariagab@gmail.com

1. INTRODUCTION

Along with the increasing advancement of technology and the development of science, the ability to analyze the needs of instrumentation or equipment and supplies that vary and are mushrooming in industry will be more sophisticated, optimal and actual [1], [2]. In the industrial sector, many tools are used to support the production process, especially in the utilization of substances that can flow or fluids [3]-[5].

In several industries such as chemical, paper, mineral processing, oil, gas, etc., accurate flow measurement and control is an important task. Venturimeter has emerged as one of the most accurate devices for measuring fluid flow rate [6]-[8]. Venturimeter is a device used to measure the flow rate of fluid flowing through a pipe. It is based on the principle of Bernoulli's equation. Bernoulli's principle which investigates the behavior of an ideal fluid flowing through a pipe states that when a fluid flows rapidly through a narrow section, the pressure in the fluid will decrease [9], [10].

A venturimeter consists of a short length of pipe in the form of a vena contracta, or the section with the least cross-sectional area that fits into a normal pipe path [11], [12]. The obstruction causes fluid flow in the throat of the venturi to produce a local pressure drop in the region that is proportional to the rate of discharge [11]-[13]. The amount of fluid flow in a venturimeter can be determined in two ways, namely by method A and method B. Method a is a measurement of the amount of flow that requires determining the pressure difference or velocity of a cross-section [14]. Method B requires determining the volume that passes through a cross-section in a certain time interval. Measuring the amount of flow in a venturimeter using method A is often found in practice questions. In addition, measurements can also be done in the laboratory [15]-[17].

Nowadays it is necessary to perform flow meter calibration test to know the accuracy of the instrument. This can be done by calculating the venturi discharge coefficient. Although experimental procedures offer good results, they often take longer time [16]-[18]. Therefore a more sophisticated method to test flow meters is through numerical methods that allow to obtain more accurate results in a shorter time compared to experimental procedures. After that, these results can be compared with previous experimental results to calibrate the instrument.

Several previous studies have discussed the effect of geometry variations on fluid flow characteristics, such as those conducted in the numerical analysis of the diameter of the V-ribbed perforated hole in a rectangular channel that shows a pressure drop, as well as a comparative study of pressure in venturi pipes with different diameters [19]-[21]. Both studies focus on pressure changes due to variations in channel or pipe dimensions, but have not integrated other technical parameters that are directly related to the performance of fluid measuring instruments. This study is here to fill this gap by conducting a numerical analysis of the flow through a venturimeter with variations in neck size, in order not only to see the pressure drop, but also to determine the velocity coefficient which is an important indicator in the validation and design of flow rate measuring instruments [22]-[24]. Thus, this study not only broadens the scope of fluid mechanics studies from a geometric perspective, but also adds a contribution to the accuracy of fluid measurement in engineering and industrial applications [25], [26].

This study presents a novelty by combining pressure drop analysis and velocity coefficient calculation in a venturimeter system through an integrated numerical approach [27], [28]. Different from previous studies that only discussed the effect of geometry variation on pressure changes, this study specifically examines the effect of venturimeter neck size variation on quantitative and functional hydrodynamic parameters on the performance of fluid measuring instruments. Through numerical simulation, this study provides a more in-depth visual representation and analytical data on the pressure and velocity distribution along the venturimeter profile. Thus, the results of this study contribute directly to the optimization of venturimeter design to improve the accuracy of fluid flow rate measurement in engineering and industrial applications [27]-[29].

This research provides important contributions in the field of fluid engineering and flow measurement instrument design, especially in improving the efficiency and accuracy of venturimeters [30]-[32]. The results of numerical analysis of the variation of the venturimeter neck size can be the basis for consideration in designing a more precise fluid discharge measurement system. In addition, this research can also be used as a reference in the development of fluid monitoring systems in industrial sectors such as energy, manufacturing, and fluid distribution systems, thus having an impact on operational efficiency and energy savings.

In the modern industrial era that demands high efficiency and precise measurement accuracy, the use of measuring instruments such as venturimeters is very vital [33], [34]. However, until now there have been few studies that numerically examine the effect of neck size variations on the velocity coefficient and pressure drop simultaneously. Lack of understanding of the relationship between venturimeter dimensions and flow characteristics can cause errors in measuring fluid discharge. Therefore, this study is urgently needed as an effort to fill the scientific gap and answer the industry's need for a more optimal and accurate venturimeter design [35], [36].

This study aims to analyze the effect of variations in the size of the venturimeter neck on the distribution of pressure and fluid flow velocity numerically, and to determine the values of the velocity coefficient and pressure drop that occur. Through a numerical simulation approach, this study also aims to provide recommendations for a more effective venturimeter design in increasing the accuracy of fluid flow rate measurements. Therefore, to find out the actual venturimeter, the author conducted a study entitled: Numerical Analysis of Flow Through a Venturimeter With Variations in Neck Size to Determine the Velocity Coefficient and Pressure Drop.

2. RESEARCH METHOD

This research is a literature study that contains the results of previous research related to the research being carried out. The materials used as literature materials are books and journals. Books related to the research being carried out by obtaining the necessary theories. The journals taken are also journals related to the research process, both national and international journals.

This study uses a simulation model using SolidWorks 2014 software. The model to be designed is a venturimeter accompanied by a manometer. To design a venturimeter design, the first step is to turn on the computer to be used, then open the SolidWorks 2014 software. After the software is open, click New Document in the upper right corner, select Part, then click OK. Next, select Insert on the menu bar, then select Sketch and select the Right Plane section as the work area. The venturimeter design to be tested has the following specifications: inlet and outlet diameter 48 mm, inlet and outlet length 125.80 mm, convergent channel length 52.20 mm, throat length 30 mm, throat diameter 10 mm, divergent length 20 mm, and thickness 4 mm. In addition, the variation in the size or neck of the venturimeter used has a throat length of 30 mm and a throat diameter of 10 mm. After the specifications are determined, the design process can be continued by drawing and setting the dimensions according to the parameters set in the SolidWorks 2014 software.

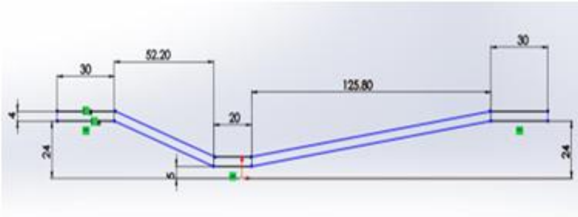

Figure 1. Venturimeter design and dimensions

After the venturimeter design is complete, select features then select Revolved Boss/base.

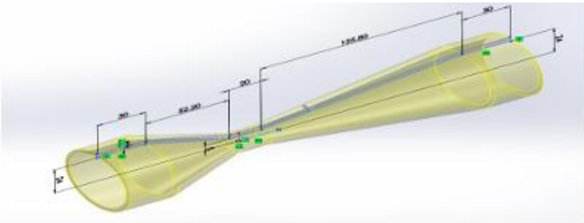

Figure 2. Venturimeter design after revolved boss/base.

The dimensions of the venturimeter with a neck diameter variation of 10mm and a length of 30mm are as follows:

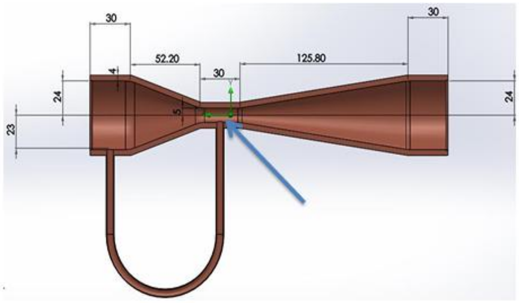

Figure 3. Venturimeter with a diameter of 10mm and a neck length of 30mm.

The following is a picture of the various neck sizes.

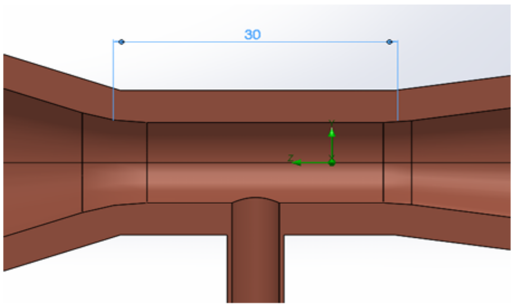

Figure 4. Venturimeter neck with a diameter of 10 mm and a neck length of 30 mm

In addition, the size of the venturimeter with a neck diameter variation of 10mm and a length of 30mm is as follows:

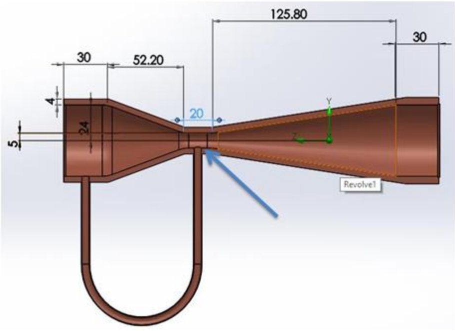

Figure 5. Venturimeter with a diameter of 10mm and a neck length of 20mm.

The following is a picture of the various neck sizes :

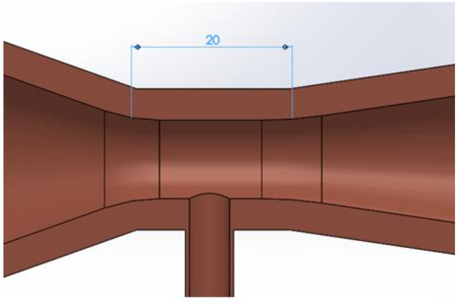

Figure 6. Venturimeter neck with a diameter of 10mm and a neck length of 20mm.

Next, create a manometer design on the venturimeter. The venturimeter to be simulated has a manometer, the design and size of the manometer are, the outer diameter of the manometer is 6 mm, the inner diameter of the manometer is 5 mm, and the height of the manometer on the inlet side is 60 mm.

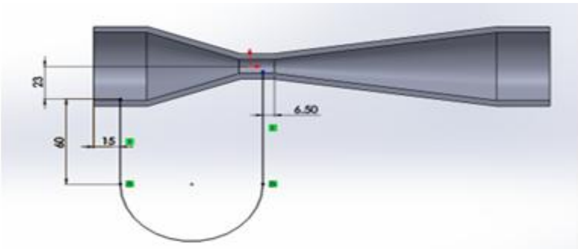

Figure 7. Manometer Design and Size

After the manometer design on the venturimeter is complete, select features then select Revovid boss/base

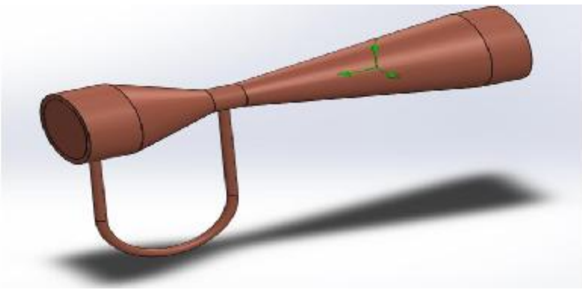

Figure 8. Manometer design after Revolved Boss/base

The testing procedure in the simulation using SolidWorks 2014 software is carried out in several steps. First, select Flow Simulation on the menu bar, then select Wizard on the Flow Simulation submenu. Next, determine the fluid that will be flowed through the venturimeter for simulation, where in this study water with a temperature of 25°C or 298 K was chosen. After that, enter the roughness value on the inner surface of the venturimeter, which in this study used copper material with a surface roughness level of 1.5 micrometers.

Table 1. Pipe Surface Roughness Value (Ɛ)

No.	Material	Ft	M
1.	Riveted Steel	0,003 - 0,03	0,0009 – 0,009
2.	Concrete	0,001 – 0,01	0,0003 – 0,003
3.	Wood Stave	0,0006 – 0,03	0,0002 – 0,0009
4.	Cast Iron	0,00085	0,00026
5.	Galvanized Iron	0,0005	0,00015
6.	Asphalted Cast Iron	0,0004	0,0001
7.	Commercial Steel or Wrought Iron	0,00015	0,000046
8.	Drawn Brass or Copper Tubing	0,000005	0,0000015
9.	Glass and Plastic	“smooth”	“smooth”

After determining the fluid and surface roughness of the venturimeter, the next step in the testing procedure is to enter the fluid inlet temperature value. Next, select the Boundary Conditions menu on the left submenu, then enter the fluid inlet velocity value and click on the venturimeter inlet side. After that, in Boundary Conditions, select Environment Pressure to determine the direction of the fluid flow, then click on the venturimeter outlet section, with this study using the Reynolds Number (Re) value in the range of 1000 to 5000. The next step is to select Goals on the left submenu to obtain the results of the simulated test data, where in this study Total Pressure was selected as the observed parameter. After all parameters are entered, click Run on the top menu bar to run the simulation. After the Running process is complete, select the Result menu, then click Cut Plot to display the color variations of the flow on the venturimeter, which depend on the Goals that have been determined before the Run process begins. If you want to display the flow shape in the venturimeter, select the Flow Trajectories menu, then click on the venturimeter inlet section. Finally, experiment with variations in the venturimeter neck size and variations in Re values from 1000 to 5000 to obtain more comprehensive results.

3. RESULTS AND DISCUSSION

The results of the simulation of pressure fluctuation research on the inlet and throat sides of the venturimeter using Solidworks 2014 software are presented in 2 variations of the neck size on the venturimeter and 5 variations of the Reynolds number. The following are the results of the pressure fluctuation simulation grouped based on the variation of the neck size on the venturimeter and the Reynolds number.

3.1. Result

The first variation is to use a Reynolds number value of 1000. To determine the velocity value of this flow variation, the following calculation can be done.

$$Re = \frac{v . d}{\vartheta} \quad \text{... (1)}$$

$$1000 = \frac{v . 0{,}048}{0{,}893 \times 10^{-6}}$$

$$1000 = \frac{v . 4{,}8 \times 10^{-2}}{8{,}93 \times 10^{-7}}$$

$$1000 = \frac{v . 4{,}8 \times 10^{-2} x\ 10^{-7}}{8{,}93}$$

$$1000 = 53751{,}339 . v$$

$$v = \frac{1000}{53751{,}399}$$

$$v = 0{,}0186 \text{ m/s}$$

The boundary conditions used for this simulation process are for the inlet velocity value of 0.0186 m/s, and the temperature value at environmental pressure is 298 K. So the simulation results are as follows.

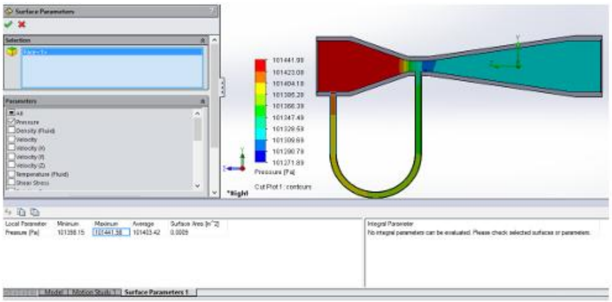

Figure 9. Pressure Drop Visualization with a diameter of 10mm and a neck length of 20m at a Reynolds Number of 1000 with Maximum h1

Simulation with a Reynolds number value of 1000 shows that in the image there is a difference in height h1 and h2 on the U manometer. At maximum h1 the pressure value recorded at that point is 101441.98 Pa and at minimum h2 the pressure value recorded at that point is 101331.17 Pa.

Since the pressure value of each point has been obtained, to obtain the ΔP value that will be used for further calculations, it can be done by subtracting the maximum h1 pressure value from the minimum h2 pressure value (101441.98-101331.17) so that the ΔP value is 110.81 Pa which can then be calculated to find the Δh value by converting units. In addition, the discharge value (Q) is also calculated. However, previously to find the discharge value, the value of the cross-sectional area must first be known (A1 on the venturimeter inlet channel and A2 on the throat channel). The calculation of the Δh, A1 and A2 values and Q. Then, after the two values are obtained from the calculation above, a calculation can be made to find the value of the velocity coefficient (c) which will be used for the graph comparison.

After conducting simulations on variations of neck diameter of 10mm and length of 30mm, the following pressure results were obtained.

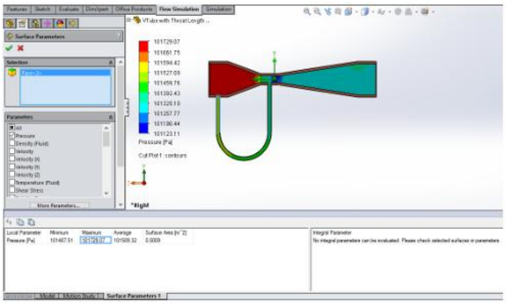

Figure 10. Pressure Drop Visualization with a diameter of 10mm and a neck length of 30mm at a number of 200 with a maximum h1

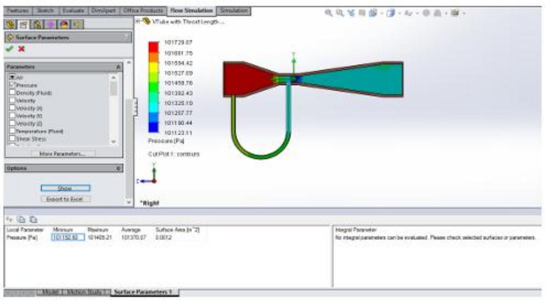

Figure 11. Pressure Drop Visualization with a diameter of 10mm and a neck length of 30mm at a Reynolds number of 2000 with a minimum h2

From the explanation listed in the simulation results of Figures 4.7 and 4.8, it is stated that the maximum pressure at h1 is 101729.07 Pa. Meanwhile, the minimum pressure at h2 is 101192.60 Pa. The difference between the two pressures (ΔP) is 536.47 Pa so that the value of Δh can be determined. which results in 0.0196 3m. Then to find the value of the velocity coefficient (c) can be done because the value of ΔP and the value of Q are already known. with the result of 3.2869.

3.2. Discussion

After all calculations have been done, the results of the simulation calculations obtained can be displayed in the form of a comparison graph. From the graph it can be concluded that all types of simulated fluid flows are interrelated. Some of the graphs displayed include:

Table 2. Comparison Value of Reynolds Graph against Pressure Drop

Reynolds	ΔP1 (Pa)	ΔP2 (Pa)
1000	110.81	136,37
2000	418.24	536,47
3000	932.52	1196,44
4000	1662.82	2133,12
5000	2588.16	3302,22

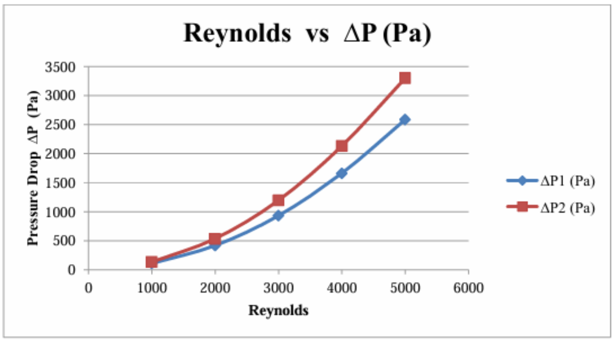

Figure 12. Reynolds Fluctuation Graph Against Pressure Drop

From the comparison graph between the Reynolds number value and Pressure Drop, it can be concluded that the cause of the increase in the Pressure Drop value is due to the increasing velocity value entering the inlet channel. Meanwhile, the increasing velocity value is due to the increasing Reynolds number. In other words, if the Reynolds number value is higher, it will cause a domino effect on other parameters on the venturimeter. ΔP1 is a venturimeter with a neck length of 20mm and a neck diameter of 10mm. ΔP2 is a venturimeter with a neck length of 30mm and a neck diameter of 10mm. The graph clearly shows the difference that ΔP1 has a smaller pressure drop because the venturimeter neck length is larger than ΔP2.

Table 3. Comparison Values in the Flow Rate Graph Against Velocity Coefficient

Q (m^3/s)	Velocity Coefficient (c1)	Velocity Coefficient (c2)
0.03365	0.90836	3,2825
0.0673	0.9351	3,2869
0.10095	0.93935	3,3144
0.1346	0.93979	3,3193
0.16825	0.93994	3,3299

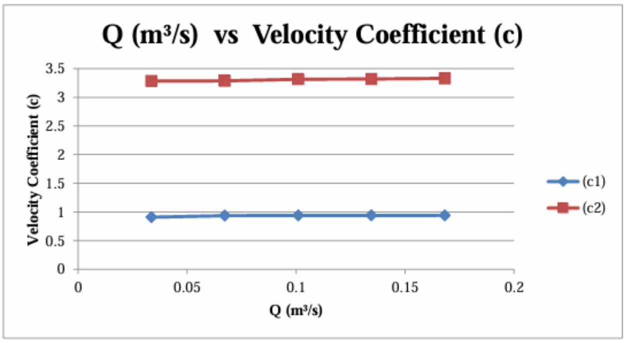

Figure 13. Flow Rate Fluctuation Graph Against Velocity Coefficient

Figure 13 shows that there is a difference in the velocity coefficient value for each diameter and length of the venturimeter neck. At a neck size with a length of 30mm, it is concluded that the velocity coefficient value is greater than the length of 20mm. This is because the smaller neck length will affect the flow that will pass through the venturimeter neck, resulting in a decrease in pressure. In this simulation, the discharge value depends on the magnitude of the velocity value at the inlet channel, the higher the incoming velocity, the higher the discharge value produced. Automatically, this also affects the resulting velocity coefficient value. Thus, if the pressure drop value is greater, the resulting velocity coefficient value will also increase.

Table 4. Comparison Values on Flow Rate Graph against Pressure Drop

Q (m^3/s)	ΔP1 (Pa)	ΔP2 (Pa)
0.03365	110.81	136,37
0.0673	418.24	536,47
0.10095	932.52	1196,44
0.1346	1662.82	2133,12
0.16825	2588.16	3302,22

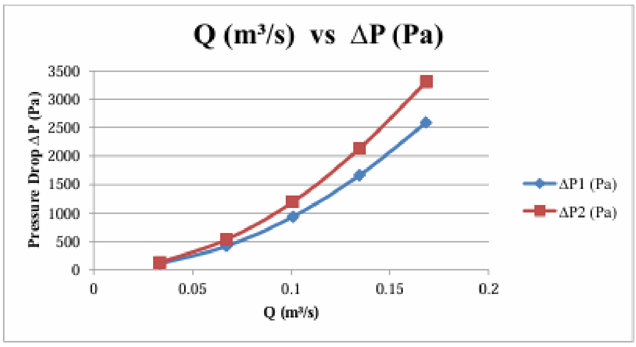

Figure 14. Flow Rate Fluctuation Graph Against Pressure Drop

From the comparison graph in Figure 14, it is known that the pressure drop value for each variation is different. This is because the length of the venturimeter neck in both variations has been enlarged in length. Venturimeter variations with smaller lengths will produce smaller pressure drop values compared to venturimeters with larger neck lengths. This is due to the long duration of the flow that will pass through the venturimeter neck. So it can be concluded that the larger the length of the venturimeter neck, the longer the time required for the fluid to pass through the venturi neck so that the pressure drop will clearly be greater compared to the smaller venturimeter neck length.

From the findings and discussion of this study. There are several previous studies that have been conducted that have led to a gap analysis of this study. The findings in this study indicate that the higher the Reynolds number value, the greater the pressure drop that occurs. In addition, variations in the length of the venturimeter neck have also been shown to affect the magnitude of the pressure drop and the fluid flow formed. In general, a longer venturimeter neck causes a more significant pressure drop due to a longer flow time duration. This study provides a practical contribution to the efficiency of fluid measuring instrument design, especially venturimeters. In previous research conducted in 2017 [37], [38] there was a fairly prominent gap when compared to this study. Previous research conducted in 2017 focused on examining the effect of the blade angle on the swirling jet diffuser and grille on the distribution of temperature and air velocity in a conditioned space, providing an important perspective on how flow direction and temperature distribution can be influenced by blade design, but did not discuss the pressure aspect or the velocity coefficient in detail as the main focus in the first article. On the other hand, this study has not touched on the influence of blade orientation or angle on flow efficiency, whereas in an article conducted in 2017 it was known that the blade angle greatly affects the distribution of speed and temperature in a closed flow system. This opens up opportunities for the development of venturimeter research towards optimizing the shape and angle of the blade in order to increase a more even and efficient flow distribution.

The gap is also seen in the research conducted by Arwizet Karudin () which discusses the flow analysis on horizontal wind turbine rotors with a numerical approach using ANSYS FLUENT [39], [40]. The study presents a more complex study of flow phenomena such as lift and drag forces, the use of turbulence models such as k-ε standard and Spalart-Allmaras, and 3D simulations on various geometric parameters. When compared to this study, it has not explored these aspects in depth, so that there is a significant methodological gap [41], [42]. The use of turbulence models and three-dimensional domains in Arwizet's study is able to provide more accurate and comprehensive simulation results, while this study is still limited to a 2D simulation approach and does not test the effects of turbulence explicitly.

This study offers novelty by presenting a new approach in analyzing fluid flow in a venturimeter by integrating the variation of the blade angle as an additional variable, using three-dimensional CFD-based numerical simulations, and applying a turbulence model to map the pressure and velocity distribution more accurately [43], [44]. In addition, this study also explores aerodynamic aspects such as lift and drag that have not been widely discussed in previous venturimeter studies, thus providing a significant contribution in optimizing the design of a more precise and efficient fluid flow measuring instrument.

This research provides important implications in the field of fluid engineering, especially in the design and development of flow measuring instruments such as venturimeters. By analyzing the effect of variations in the size of the venturimeter neck on the pressure drop and velocity coefficient through numerical simulation, the results of this study can be used as a basis for optimizing the design of a more efficient and accurate venturimeter [45]-[47]. In addition, the numerical approach used opens up opportunities for the application of simulation methods as a faster and more cost-effective alternative compared to conventional experiments [48], [49]. If further developed by considering additional variables such as blade angles or turbulence models, this research can also contribute to the development of fluid flow measurement systems for various industrial needs, such as HVAC systems, energy, and process engineering.

This study has several limitations that need to be considered for further development. First, the simulations conducted are still limited to two-dimensional (2D) models using SolidWorks software, so they are not yet able to represent the full spatial flow distribution as can be captured through three-dimensional modeling [50]-[52]. This limitation has an impact on the accuracy in visualizing the complex interactions between flow variables, especially in critical areas such as the inlet, throat, and outlet of the venturimeter. Second, this study has not explicitly considered the effects of turbulence, either through the selection of a turbulence model or variations in complex turbulent flow structures, even though turbulence phenomena play an important role in determining the behavior of pressure and flow velocity in fluid systems [53], [54]. Third, the geometric design of the venturimeter studied does not include the influence of the blade angle or other more complex geometric shapes, even though previous studies have shown that these variables have a significant effect on the distribution of velocity, pressure, and flow efficiency. Finally, the simulation results obtained have not been validated with real experimental data, so the level of reliability and accuracy of the numerical model used still needs to be tested further to ensure compliance with actual conditions in the field.

As a follow-up to the findings and limitations of this study, it is recommended that further studies conduct simulations in a three-dimensional (3D) domain to obtain more realistic flow visualizations, and integrate turbulence models such as the standard k-ε or Spalart-Allmaras to accurately capture turbulent flow characteristics. In addition, new design variables such as blade angle, inlet and outlet shapes, and pipe materials need to be added to evaluate their effects on venturimeter performance [55]-[57]. Validation of simulation results with experimental data is also important to strengthen the reliability of the numerical model. The development of multi-parameter-based simulations, such as variations in working fluids and operating temperatures, is also recommended so that the research results are more applicable in various industrial conditions [58]-[60].

4. CONCLUSION

Based on the simulation results and discussion, it can be concluded that the greater the fluid velocity entering through the inlet channel, the greater the Reynolds number, flow rate, and pressure drop produced. In testing with variations in Reynolds numbers from 1000 to 5000, there was a fluctuation in the height difference in the U manometer, where the height value at each point was obtained by converting units from Pa to mH_2O. In addition, in simulations with variations in the size of the venturimeter neck, it is known that the longer the venturimeter neck, the greater the pressure drop that occurs due to the longer duration of fluid flow. The resulting velocity coefficient is highly dependent on the fluid inlet velocity through the venturi pipe inlet, where the greater the inlet velocity, the greater the resulting flow rate. Thus, changes in one parameter, such as the velocity or length of the venturimeter neck, will affect other parameters in the fluid flow system.

ACKNOWLEDGEMENTS

Thank you to all parties who have provided support, assistance, and motivation in completing this research. Thanks are also conveyed to colleagues who have shared knowledge, advice, and enthusiasm during the research process. Hopefully the results of this research can be useful and contribute to the development of science.

REFERENCES

[1] R. Hilala, L. A. R. Laliyo, J. La Kilo, J. S. Tangio, E. Mohamad, and M. Sihaloho, "Measuring students' scientific argumentation skills in explaining phenomena related to acid-base concepts," *J. Pendidik. Sains Indones.*, vol. 11, no. 2, pp. 360–378, 2023, doi: 10.24815/jpsi.v11i2.27822.

[2] A. B. T. Penzlin, W. Kley, and R. P. Nelson, "Parking planets in circumbinary discs," *Astron. Astrophys.*, vol. 645, p. A68, 2021, doi: 10.1051/0004-6361/202039319.

[3] M. Muliana, H. Nufus, N. Nuraina, N. Mahyuni, and A. Husna, "Developing numeracy module based on local culture in Indonesia," *J. Elem.*, vol. 9, no. 1, pp. 168–182, 2023, doi: 10.29408/jel.v9i1.6883.

[4] J. Rodríguez-Arce, E. Vázquez-Cano, J. P. Cobá Juárez-Pegueros, and S. González-García, "Comparison of learning content representations to improve L2 vocabulary acquisition using m-learning," *SAGE Open*, vol. 13, no. 4, pp. 1–15, 2023, doi: 10.1177/21582440231216819.

[5] A. U. H. Prabu Wisnu Puji Wibowo, Leli Indriyani, Muhammad Hanif Abdurrahman, "Menelaah para oknum yang tidak bijak dalam menggunakan media sosial atau cyberspace," *Kult. J. Ilmu Hukum, Sos. dan Hum.*, vol. 1, no. 5, pp. 320–

330, 2023, doi: 10.572349/kultura.v1i5.565.
[6] B. Sun, C. E. Loh, and Y. Nie, “The COVID-19 school closure effect on students’ print and digital leisure reading,” *Comput. Educ. Open*, vol. 2, p. 100033, 2021, doi: 10.1016/j.caeo.2021.100033.
[7] Asmayawati, Yufiarti, and E. Yetti, “Pedagogical innovation and curricular adaptation in enhancing digital literacy: A local wisdom approach for sustainable development in Indonesia context,” *J. Open Innov. Technol. Mark. Complex.*, vol. 10, no. 1, p. 100233, 2024, doi: 10.1016/j.joitmc.2024.100233.
[8] Y. Su *et al.*, “Printable, highly sensitive flexible temperature sensors for human body temperature monitoring: A review,” *Nanoscale Res. Lett.*, vol. 15, no. 1, 2020, doi: 10.1186/s11671-020-03428-4.
[9] Y.-D. Tsai, D. Farnocchia, M. Micheli, S. Vagnozzi, and L. Visinelli, “Constraints on fifth forces and ultralight dark matter from OSIRIS-REx target asteroid Bennu,” *Commun. Phys.*, vol. 7, no. 1, pp. 1–7, 2023, doi: 10.1038/s42005-024-01779-3.
[10] H. R. Ganesha and P. S. Aithal, “How to choose an appropriate research data collection method and method choice among various research data collection methods and method choices during ph.d. program in India?,” *Int. J. Manag. Technol. Soc. Sci.*, vol. 7, no. 2, pp. 455–489, 2022, doi: 10.47992/ijmts.2581.6012.0233.
[11] R. Pečenko, T. Hozjan, and S. Huč, “A new numerical model for analysing timber-concrete composite beams under fire conditions,” *Structures*, vol. 75, no. January, p. 108575, 2025, doi: 10.1016/j.istruc.2025.108575.
[12] K. Parach, B. Jafari, and K. Hosseinzadeh, “Numerical analysis of integrated photovoltaic thermal systems utilizing nanoparticles with phase change material and fin attachments,” *Int. J. Thermofluids*, vol. 27, no. April, p. 101210, 2025, doi: 10.1016/j.ijft.2025.101210.
[13] K. Mardiana, A. Mickovska-Raleva, and J. M. Zakari, “A comparative study: Attitudes and thinking patterns students in citizenship education,” *J. Soc. Knowl. Educ.*, vol. 5, no. 3, pp. 106–112, 2024, doi: 10.37251/jske.v5i3.1072.
[14] L. Nurnaningsih and G. Prahmana, Rully Charitas Indra Prahmana, Wahid Yunianto, “The integration of Ethno-RME in MatCityMap application to support students’ learning of system of linear equations: A case of Mangkujo Math Trail,” *J. Honai …*, vol. 7, no. April, pp. 155–176, 2024, doi: 10.30862/jhm.v7i1.599.
[15] A. SHEHENAZ ADAM, “Exploring ethnomathematics in the Maldives: Counting and measuring,” *Maldives Natl. J. Res.*, vol. 8, no. 2, pp. 7–30, 2020, doi: 10.62338/epe8ay39.
[16] H. V. Saphira, “Integrating Local Wisdom-Based Learning To Preparing The Pancasila Students’ Profile, Yes or No?,” *Int. J. Curr. Educ. Res.*, vol. 1, no. 1, pp. 18–35, 2022, doi: 10.53621/ijocer.v1i1.136.
[17] M. S. Hsu, C. L. Yeh, S. J. Cheng, and C. P. Lin, “Integrating digital technologies in dental technician education: A comparative study of national examination in Asian countries,” *J. Dent. Sci.*, vol. 20, no. 1, pp. 28–35, 2024, doi: 10.1016/j.jds.2024.10.017.
[18] M. Moghadas, A. Fekete, A. Rajabifard, and T. Kötter, “The wisdom of crowds for improved disaster resilience: a near-real-time analysis of crowdsourced social media data on the 2021 flood in Germany,” *GeoJournal*, vol. 88, no. 4, pp. 4215–4241, 2023, doi: 10.1007/s10708-023-10858-x.
[19] D. U. Iswavigra and L. Endriani Zen, “Systematic literature review: pengaplikasian metode VIKOR dalam decision upport system,” *J. Inf. dan Teknol.*, vol. 5, no. 3, pp. 13–19, 2023, doi: 10.60083/jidt.v5i3.379.
[20] N. V. Antonova, Z. N. Shmeleva, and N. S. Kozulina, “Lifelong learning as the way of modern personality development in Russia on the example of higher educational institution of technical and natural-scientific profile,” *J. Phys. Conf. Ser.*, vol. 1691, no. 1, 2020, doi: 10.1088/1742-6596/1691/1/012146.
[21] B. Liu and J. Ji, “A tale of planet formation: From dust to planets,” *Res. Astron. Astrophys.*, vol. 20, no. 10, 2020, doi: 10.1088/1674-4527/20/10/164.
[22] X. Wang, D. Chen, G. Pang, S. A. Anwar, T. Ou, and M. Yang, “Effects of cumulus parameterization and land-surface hydrology schemes on tibetan plateau climate simulation during the wet season: insights from the RegCM4 model,” *Clim. Dyn.*, vol. 57, no. 7–8, pp. 1853–1879, 2021, doi: 10.1007/s00382-021-05781-1.
[23] R. Buhumaid *et al.*, “Professionalism-training in undergraduate medical education in a multi-cultural, multi-ethnic setting in the Gulf Region: an exploration of reflective essays,” *BMC Med. Educ.*, vol. 24, no. 1, pp. 1–18, 2024, doi: 10.1186/s12909-024-05103-z.
[24] R. Angraini and F. Rakhmawati, “Ethnomathematics Exploration of Fish Trader Activities in The Traditional Market of Punggulan Village, Asahan Regency,” *Indones. J. Sci. Math. Educ.*, vol. 6, no. 2, pp. 213–226, 2023, doi: 10.24042/ijsme.v6i2.17182.
[25] K. Aliyi Koroche, “Numerical solution of first order ordinary differential equation by using runge-kutta method,” *Int. J. Syst. Sci. Appl. Math.*, vol. 6, no. 1, p. 1, 2021, doi: 10.11648/j.ijssam.20210601.11.
[26] E. Fiandrini *et al.*, “Numerical modeling of cosmic rays in the heliosphere: Analysis of proton data from AMS-02 and PAMELA,” *Phys. Rev. D*, vol. 104, no. 2, p. 23012, 2021, doi: 10.1103/PhysRevD.104.023012.
[27] J. W. Lee, K. J. Jung, and Y. J. Kim, “Numerical analysis on performance of induced gas flotation machine using MUSIG model,” *Eng. Appl. Comput. Fluid Mech.*, vol. 14, no. 1, pp. 778–789, 2020, doi: 10.1080/19942060.2020.1771426.
[28] J. Bakunowicz and T. Kopecki, “Global analysis of the aircraft structure and its application to the preliminary design stage,” *Aviation*, vol. 9, no. 3, pp. 29–35, 2005, doi: 10.1080/16487788.2005.9635908.
[29] P. A. Akimov, M. L. Mozgaleva, and T. B. Kaytukov, “Numerical solution of the problem of beam analysis with the use of b-spline finite element method,” *Int. J. Comput. Civ. Struct. Eng.*, vol. 16, no. 3, pp. 12–22, 2020, doi: 10.22337/2587-9618-2020-16-3-12-22.
[30] S. A. Hemmerling *et al.*, “Elevating local knowledge through participatory modeling: active community engagement in restoration planning in coastal Louisiana,” *J. Geogr. Syst.*, vol. 22, no. 2, pp. 241–266, 2020, doi: 10.1007/s10109-019-00313-2.
[31] M. Maswar, “Analisis statistik deskriptif nilai uas ekonomitrika mahasiswa dengan program spss 23 & eviews 8.1,” *J. Pendidik. Islam Indones.*, vol. 1, no. 2, pp. 273–292, 2017, doi: 10.35316/jpii.v1i2.54.
[32] I. Hacking, “Scoping studies: advancing the methodology,” *Represent. Interv.*, pp. 1–18, 2012, doi:

10.1017/cbo9780511814563.003.
[33] M. Carmona, J. Llain, J. Sandoval, L. Beltrán, D. Acosta, and V. Pugliese, "Numerical analysis of the combustion in a micromix-type burner operating with hydrogen-natural gas blends," *Appl. Therm. Eng.*, vol. 272, no. April, pp. 30–31, 2025, doi: 10.1016/j.applthermaleng.2025.126336.
[34] J. Zhang, L. Zhang, B. Zhang, N. Zhou, L. Lei, and B. Li, "Numerical analysis and experimental study of two-phase flow pattern and pressure drop characteristics in internally microfin tubes," *Case Stud. Therm. Eng.*, vol. 64, no. November, p. 105521, 2024, doi: 10.1016/j.csite.2024.105521.
[35] Z. Huang *et al.*, "Numerical analysis of asymmetric biomimetic flow field structure design for vanadium redox flow battery," *Futur. Batter.*, vol. 5, no. November 2024, p. 100017, 2025, doi: 10.1016/j.fub.2024.100017.
[36] F. Ullah and M. B. Ashraf, "Numerical heat transfer analysis of Carreau nanofluid flow over curved stretched surface with nonlinear effects and viscous dissipation," *Int. J. Thermofluids*, vol. 24, no. October, 2024, doi: 10.1016/j.ijft.2024.100914.
[37] Y. Tu, H. Lin, M. Chen, Z. Zhang, W. Cai, and Z. Zhu, "Design and numerical analysis of a Y-shaped flow channel for enhanced hydrogen production in solid oxide electrolysis cells," *Int. J. Electrochem. Sci.* , vol. 19, no. 11, p. 100806, 2024, doi: 10.1016/j.ijoes.2024.100806.
[38] L. O. Aselebe *et al.*, "Numerical analysis of Au/Blood aggregate nanofluid flow enclosed under the influence of magnetic field and thermal radiation," *Results Mater.*, vol. 24, no. August, p. 100631, 2024, doi: 10.1016/j.rinma.2024.100631.
[39] D. J. Jasim, M. sabah mahdi, O. S. Mahdy, A. Basem, S. H. H. Karouei, and M. Alinia-kolaei, "Hydrothermal analysis of hybrid nanofluid flow inside a shell and double coil heat exchanger; Numerical examination," *Int. J. Thermofluids*, vol. 23, no. July, p. 100770, 2024, doi: 10.1016/j.ijft.2024.100770.
[40] M. N. Fares *et al.*, "Two-phase analysis of heat transfer of nanofluid flow in a wavy channel heat exchanger: A numerical approach," *Int. J. Thermofluids*, vol. 23, no. July, p. 100786, 2024, doi: 10.1016/j.ijft.2024.100786.
[41] F. N. M. Elwekeel and A. M. M. Abdala, "Numerical analysis of the heat transfer performance of the absorber tube of a parabolic trough solar collector using the swirling flow technique," *Case Stud. Therm. Eng.*, vol. 60, no. July, p. 104801, 2024, doi: 10.1016/j.csite.2024.104801.
[42] I. Catanzaro *et al.*, "Numerical structural analysis and flow-induced vibration study in support of the design of the EU-DEMO once-through steam generator mock-up for the STEAM experimental facility," *Fusion Eng. Des.*, vol. 209, no. August, pp. 1–13, 2024, doi: 10.1016/j.fusengdes.2024.114698.
[43] C. Yang, Y. bo Tie, X. zheng Zhang, Y. feng Zhang, Z. jie Ning, and Z. liang Li, "Analysis of debris flow control effect and hazard assessment in Xinqiao Gully, Wenchuan Ms 8.0 earthquake area based on numerical simulation," *China Geol.*, vol. 7, no. 2, pp. 248–263, 2024, doi: 10.31035/cg2023144.
[44] M. J. Alshukri, R. F. Hamad, A. A. Eidan, and A. Al-Manea, "Convective heat transfer analysis in turbulent nanofluid flow through a rectangular channel with staggered obstacles: A numerical simulation," *Int. J. Thermofluids*, vol. 23, no. July, p. 100753, 2024, doi: 10.1016/j.ijft.2024.100753.
[45] M. Ableidinger, E. Buckwar, and H. Hinterleitner, *A Stochastic Version of the Jansen and Rit Neural Mass Model: Analysis and Numerics*, vol. 7, no. 1. The Author(s), 2017. doi: 10.1186/s13408-017-0046-4.
[46] M. Elshabrawy, M. A. Abdeen, and S. Beshir, "Analytic and numeric analysis for deformation of non-prismatic beams resting on elastic foundations," *Beni-Suef Univ. J. Basic Appl. Sci.*, vol. 10, no. 1, 2021, doi: 10.1186/s43088-021-00144-5.
[47] J. Saini, J. Bakshi, N. K. Panda, M. Sharma, D. Vir, and A. K. Goyal, "Cut-off points to classify numeric values of quality of life into normal, mild, moderate, and severe categories: an update for EORTC-QLQ-H&N35," *Egypt. J. Otolaryngol.*, vol. 40, no. 1, 2024, doi: 10.1186/s43163-024-00642-0.
[48] M. E. Elgack, K. Al-Souqi, M. O. Hamdan, and M. Abdelgawad, "Compressibility effects in microchannel flows between two-parallel plates at low reynolds and mach numbers: Numerical analysis," *Int. J. Thermofluids*, vol. 24, no. October, p. 100921, 2024, doi: 10.1016/j.ijft.2024.100921.
[49] C. Mistrangelo, L. Bühler, C. Courtessole, and C. Koehly, "Numerical and experimental analysis of magneto-convective flows around pipes," *Fusion Eng. Des.*, vol. 202, no. October 2023, 2024, doi: 10.1016/j.fusengdes.2024.114325.
[50] A. P. Palamides and T. G. Yannopoulos, "Terminal value problem for singular ordinary differential equations: Theoretical analysis and numerical simulations of ground states," *Bound. Value Probl.*, vol. 2006, no. August, pp. 1–28, 2006, doi: 10.1155/bvp/2006/28719.
[51] Y. Khodair and S. Hassiotis, "Numerical and experimental analyses of an integral bridge," *Int. J. Adv. Struct. Eng.*, vol. 5, no. 1, pp. 1–12, 2013, doi: 10.1186/2008-6695-5-14.
[52] L. He, L. Yi, and P. Tang, "Numerical scheme and dynamic analysis for variable-order fractional van der Pol model of nonlinear economic cycle," *Adv. Differ. Equations*, vol. 2016, no. 1, 2016, doi: 10.1186/s13662-016-0920-5.
[53] I. Kahhale, N. J. Buser, C. R. Madan, and J. L. Hanson, "Quantifying numerical and spatial reliability of hippocampal and amygdala subdivisions in FreeSurfer," *Brain Informatics*, vol. 10, no. 1, 2023, doi: 10.1186/s40708-023-00189-5.
[54] W.-E. E. Mohamed, "Assessing the effects of different foundation base shapes on settlement and heaving in expansive clay: numerical analysis," *J. Umm Al-Qura Univ. Eng. Archit.*, vol. 15, no. 4, pp. 517–528, 2024, doi: 10.1007/s43995-024-00073-1.
[55] G. Brandonisio and M. T. Naqash, "Validation of numerical results of complex seismic analysis through simple analytics," *J. Umm Al-Qura Univ. Eng. Archit.*, vol. 15, no. 2, pp. 93–111, 2024, doi: 10.1007/s43995-023-00045-x.
[56] W. Wen, S. Li, A. Yan, and J. Zeng, "Numerical analysis on the time-varying temperature field distribution patterns of ballastless track steel-concrete composite box girders at ambient temperature based on field measurements," *Adv. Bridg. Eng.*, vol. 2, no. 1, 2021, doi: 10.1186/s43251-021-00043-w.
[57] Y. Ge, L. Zheng, Z. Deng, and G. Fang, "Parametric design and numerical analysis of super long span upper-support thrust-bearing concrete arch bridge," *Adv. Bridg. Eng.*, vol. 6, no. 1, 2025, doi: 10.1186/s43251-024-00151-3.
[58] M. Kalala, P. Kisula, I. Muheme, and L. Tartibu, "Numerical analysis of a protective coating for mining industry feed

chute," *J. Eng. Appl. Sci.*, vol. 71, no. 1, pp. 1–16, 2024, doi: 10.1186/s44147-024-00452-4.
[59] H. J. Kim, K. Hwang, Y. H. Yoon, and H. J. Lee, "Numerical Analysis of the Effect of Afterburning on Damage to the Concrete Structure Under Interior Explosion," *Int. J. Concr. Struct. Mater.*, vol. 16, no. 1, 2022, doi: 10.1186/s40069-022-00497-w.
[60] H. Wang *et al.*, "Numerical investigations on the performance analysis of multiple fracturing horizontal wells in enhanced geothermal system," *Geotherm. Energy*, vol. 13, no. 1, 2025, doi: 10.1186/s40517-025-00338-5.